

Trustworthiness-Driven Graph Convolutional Networks for Signed Network Embedding

Min-Jeong Kim*, Yeon-Chang Lee*, David Y. Kang, and Sang-Wook Kim[‡], *Member, IEEE*

Abstract—The problem of representing nodes in a signed network as low-dimensional vectors, known as signed network embedding (SNE), has garnered considerable attention in recent years. While several SNE methods based on *graph convolutional networks* (GCN) have been proposed for this problem, we point out that they significantly rely on the assumption that the decades-old *balance theory* always holds in the real-world. To address this limitation, we propose a novel GCN-based SNE approach, named as TrustSGCN, which corrects for incorrect embedding propagation in GCN by utilizing the trustworthiness on edge signs for high-order relationships inferred by the balance theory. The proposed approach consists of three modules: (M1) generation of each node’s extended ego-network; (M2) measurement of trustworthiness on edge signs; and (M3) trustworthiness-aware propagation of embeddings. Furthermore, TrustSGCN learns the node embeddings by leveraging two well-known societal theories, *i.e.*, balance and status. The experiments on four real-world signed network datasets demonstrate that TrustSGCN consistently outperforms five state-of-the-art GCN-based SNE methods. The code is available at <https://github.com/kmj0792/TrustSGCN>.

Index Terms—signed networks, trustworthy graph convolutional networks, balance theory

I. INTRODUCTION

Background. In real-world networks, interactions between nodes are often *signed*, representing two contrasting relationships, such as friend/enemy and support/oppose [1]–[3]. With the advent of signed networks, we can better understand the complex relationships between nodes and measure the polarization in social discussions [4]–[9]. Motivated by such broad applicability, the problem of signed network embedding (SNE) [10], which aims to represent nodes in a given signed network as low-dimensional vectors, has increasingly attracted attention in recent years [11], [12]. The learned vectors (*i.e.*, embeddings) can be used as intrinsic features of nodes in solving various downstream tasks related to information retrieval and data mining, including link prediction [13]–[15] and recommendation [16]–[19].

In particular, with the advance of *graph convolutional networks* (GCN) [20]–[22], many GCN-based SNE methods

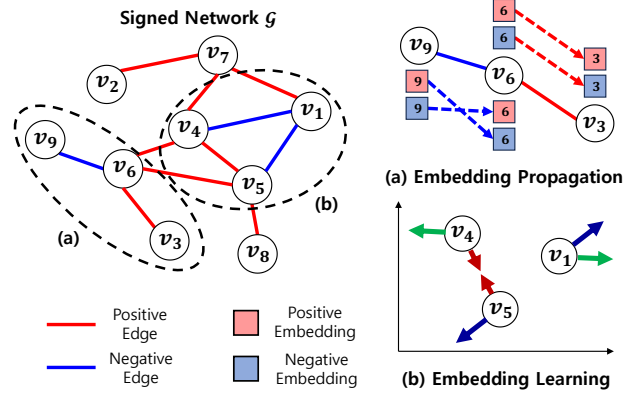


Fig. 1. The use of balance theory in existing GCN-based SNE methods.

have been proposed recently [23]–[27]. They design GCNs that can model the *homophily* nature of positive relationships and the *heterophily* nature of negative relationships in a given signed network. Furthermore, they leverage the well-known *balance theory* [28], [29] in social sciences to understand the formation of high-order signed relationships in the signed network. It states that such high-order relationships tend to form *balanced triads* that satisfy the following rules: “a friend of my friend is my friend,” “a friend of my enemy is my enemy,” “an enemy of my friend is my enemy,” and “an enemy of my enemy is my friend.”

To take advantage of the balance theory, most GCN-based SNE methods generate two types (*i.e.*, positive and negative) of embeddings for each node v_i by performing the following embedding propagation [23]–[27]: embeddings of the *same* (*resp.* *opposite*) polarity are propagated between v_i and its neighbors with *positive* (*resp.* *negative*) relationships (Figure 1-(a)). Then, they learn the node embeddings so that the likelihood of existent edges in the input signed network can be maximized. Along with this optimization, a more recent work [26], [30] additionally learns the node embeddings such that the proximities between *three nodes* incident to the balanced triads can be preserved (Figure 1-(b)). To sum up, existing GCN-based SNE methods significantly rely on the balance theory when they generate and learn node embeddings.

Motivation. However, edge relationships in real settings of signed networks often violate the rules of the balance theory [16], [31]. For instance, on platforms like Reddit¹, a social-media discussion platform, it is common to observe situations where individuals have conflicting opinions on different topics, *e.g.*, even though Bob supports Alice who opposes

M.-J. Kim is with the Department of Artificial Intelligence, Hanyang University, Seoul, South Korea. E-mail: kmj0792@hanyang.ac.kr

Y.-C. Lee is with the School of Computational Science and Engineering, Georgia Institute of Technology, Atlanta, GA, USA. E-mail: yeonchang@gatech.edu

David Y. Kang is with the School of Information, University of Michigan, Ann Arbor, MI, USA. E-mail: dyskang@umich.edu

S.-W. Kim is with the Department of Computer Science, Hanyang University, Seoul, South Korea. E-mail: wook@hanyang.ac.kr

*Two first authors have contributed equally to this work.

[‡]Corresponding author.

¹<https://www.reddit.com>

TABLE I

RATIOS OF BALANCED/UNBALANCED TRIADS. GIVEN TWO SIGNS (*i.e.*, PRIOR SIGNS) IN A TRIAD, WE CHECK WHETHER THE REMAINING SIGN (*i.e.*, POSTERIOR SIGN) SATISFIES THE BALANCE THEORY.

Triads	Prior Posterior	(+, +)		(+, -)/(-, +)		(-, -)	
		+	-	+	-	+	-
Datasets	Bitcoin-Alpha	85%	15%	63%	37%	93%	7%
	Bitcoin-OTC	86%	14%	42%	58%	94%	6%
	Slashdot	82%	18%	51%	49%	79%	21%
	Epinions	96%	4%	71%	29%	90%	10%
Balanced?		○	×	×	○	○	×

John on a specific topic (*e.g.*, politics), Bob may support John on a different topic (*e.g.*, sports). Additionally, in the context of politics, it often occurs in the United States House of Representatives that members belonging to a particular political party have no negative opinions towards bills or speeches initiated by members of the opposing party.

As a demonstration, Table I shows that a high number of *unbalanced triads*, which do not satisfy the balance theory, appear in the real-world signed network datasets. For instance, on Epinions, we can see that 71% of triads with the prior signs of (+,-) have a posterior sign of +, indicating “an enemy of my friend is my friend.” It indicates that the balance theory can bring about substantial errors in predicting the edge signs for high-order relationships when blindly employed. Consequently, the node embeddings, which learn the *incorrect edge signs* inferred by the balance theory, can adversely affect the downstream tasks.

Our Work. In this work, we aim to measure the trustworthiness on edge signs for high-order relationships inferred by balance theory and correct wrong embedding propagation based on the trustworthiness thus measured. Toward this goal, we propose a novel SNE approach, named as TrustSGCN, which learns Trustworthiness on edge signs for Signed Graph Convolutional Networks. For each node v_i in a given signed network, TrustSGCN first constructs v_i ’s extended ego-network consisting of v_i ’s direct and high-order neighbors whose trustworthiness on edge signs will be measured. With the ego network, TrustSGCN validates whether the edge signs for high-order neighbors inferred by balance theory are *trustworthy or not*. Then, TrustSGCN performs *different embedding propagation* according to trustworthy or untrustworthy edge signs, updating v_i ’s positive and negative embeddings.

Finally, TrustSGCN learns the node embeddings to preserve the proximity between nodes connected by existing edges in the embedding space. To achieve this, we incorporate not only the balance theory but also another social theory, *i.e.*, the *status theory* [32], into the learning mechanism of TrustSGCN. We experimentally demonstrate that (1) considering the trustworthiness on edge signs helps accurately preserve the proximities between nodes, (2) TrustSGCN outperforms five state-of-the-art GCN-based SNE methods [23]–[27] in terms of an edge sign prediction task, and (3) TrustSGCN requires a reasonable training time to achieve higher accuracy than competitors.

Contributions. Our contributions are summarized as follows:

- **Important Observation:** We point out that the balance theory could cause incorrect embedding propagation under

existing GCN-based SNE methods, if relied blindly on.

- **Effective SNE Approach:** We propose TrustSGCN that learns node embeddings based on trustworthiness on edge signs for signed graph convolutional networks.
 - We design three modules to facilitate embedding propagation, taking into account the trustworthiness on edge signs for high-order signed relationships.
 - We design a loss function to facilitate embedding learning while preserving the signed and directed relationships based on the balance and status theories.
- **Comprehensive Validation:** Our comprehensive validation demonstrates the effectiveness of each individual design choice in TrustSGCN, as well as the superiority of our approach achieved when all these choices are combined.

The earlier version of this manuscript was presented as a short paper (*i.e.*, conference version) [33] at ACM SIGIR 2023, featuring initial ideas and preliminary experimental results. In this extended version, we (1) provide comprehensive and detailed descriptions of our motivation, intuitions behind our ideas, and the implementation details of the proposed approach, (2) design a multi-objective loss function that jointly considers the balance and status theories, and (3) conduct more experiments to demonstrate the effectiveness of the proposed approach more clearly.

Organization. The rest of this paper is organized as follows. In Section II, we review previous studies on the SNE problem. In Section III, we present our proposed approach in detail. In Section IV, we validate the effectiveness of the proposed approach through extensive experiments. Finally, we summarize the paper in Section V.

II. RELATED WORK

In this section, we briefly review the social theories commonly used in signed network analysis (Section II-A), and then discuss how existing SNE methods take advantage of these social theories (Section II-B).

A. Social Theories for Signed Networks

Balance Theory. The balance theory [28], [29] is a concept derived from social psychology that provides insights into the intricate dynamics of human relationships. It offers an explanation for the signed relationships between three nodes in a signed undirected network.

According to the balance theory, an unknown signed relationship between two nodes v_i and v_k can be inferred from the two signed relationships known between each of the nodes and their common neighbor v_j . This inference is guided by the following rules [28], [29]: (1) a friend of my friend is my friend; (2) a friend of my enemy is my enemy; (3) an enemy of my friend is my enemy; and (4) an enemy of my enemy is my friend. In a signed network, triads that adhere to these rules are called ‘*balanced triads*’ (*i.e.*, having an even number of negative edges), while those that deviate from these rules are called ‘*unbalanced triads*’ (*i.e.*, having an odd number of negative edges). Figures 2-(a) and (b) illustrate the distinction between balanced and unbalanced triads. For instance, in Figure 2-(i), v_k , who is a friend of v_i ’s friend v_j ,

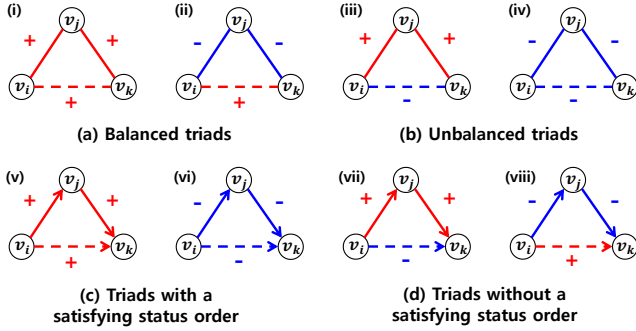


Fig. 2. Examples of triads where balance and status theories are followed and not followed

is considered as a friend of v_i , making it a balanced triad. Conversely, in Figure 2-(iii), v_k is considered as an enemy of v_i , which violates the balance theory. Three nodes v_i , v_j , and v_k are in an unbalanced triad. However, it is important to note that in real-world settings of signed networks, balance theory does not always hold, as mentioned in Section I (see Table I).

Status Theory. The status theory [32] is another theory from social psychology and is used to model *signed directed networks*. It explains the social status of nodes in signed directed networks based on the signs and directions of edges, where status can refer to the reputation, ranking, and skill level.

According to the status theory, an unknown signed and directed relationship between two nodes v_i and v_k can be inferred from the two signed and directed relationships known between each of the nodes and their common neighbors v_j . This inference is guided by the following rules [32]: (1) when a positive link exists from the source node to the destination node, the source node regards the destination node as a friend with a higher status than itself; and (2) when a negative link exists from the source node to the destination node, the source node regards the destination node as an enemy with a lower status than itself. In a signed directed network, the triads that adhere to these rules are called ‘*triads with a satisfying status order*’, while those that violate these rules are called ‘*triads without a satisfying status order*.’ Figures 2-(c) and (d) illustrate the distinction between triads with and without a satisfying status order. As in Figure 2-(v) and Figure 2-(vii), suppose v_j is a friend of v_i with a higher status than v_i , and v_k is a friend of v_j with a higher status than v_j . In this case, v_k is considered as a friend and an enemy of v_i with a higher and lower status than v_i in Figure 2-(v) and Figure 2-(vii), respectively; thus, the former and the latter represent a triad with and without a satisfying status order, respectively.

B. Signed Network Embedding Methods

SNE methods aim to represent nodes in a given signed network as low-dimensional vectors so that the vectors preserve structural and semantic properties in the network.

Traditional SNE Methods. SiNE [34], SIDE [35], and BESIDE [36] are traditional methods that leverage balance theory to learn the signed relationships between nodes. They ensure that the nodes with a positive relationship are positioned closer

to each other in the embedding space, while the nodes with a negative relationship are positioned farther apart. In addition, SIDE employs random walks based on balance theory to exploit the unknown signed relationships between nodes, while BESIDE models and learns “bridge” edges whose adjacent nodes have no common neighbors based on status theory.

GCN-based SNE Methods. Several SNE methods have been developed [34]–[36], incorporating successful convolution-based techniques [23]–[27], [37] in representation learning. First, SGCN [23], SNEA [25], and LightSGCN [37] utilize balance theory for predicting high-order signed relationships and designing their propagation strategies. As mentioned in Section I, they generate positive and negative embeddings for each node so that the embeddings of the same (resp. opposite) polarity are propagated between the nodes with positive (resp. negative) relationships. Note that SGCN is the first GCN-based SNE method. Then, SNEA adds a self-attention mechanism to SGCN, while LightSGCN simplifies the embedding propagation process by using a linear approach.

On the other hand, SIGAT [24] and SDGNN [26] jointly consider the sign and direction information of signed networks. They define motifs (e.g., $\Delta_{i,j,k}: v_i \rightarrow^+ v_j, v_i \rightarrow^+ v_k, v_k \rightarrow^+ v_j$) based on balance and status theories, and utilize motif-based Graph Attention Networks (GAT) for embedding propagation. Furthermore, SDGNN introduces loss functions that incorporate sign, direction, and triangle information. SGCL [27] enhances the embedding generation process with graph augmentations based on balance theory and additionally models the augmented signed relationships between nodes by using contrastive learning.

In summary, while most existing SNE methods successfully incorporate balance theory into their design, they face the challenge of learning the incorrect edge signs predicted by the balance theory.

III. THE PROPOSED APPROACH: TRUSTSGCN

In this section, we describe TrustSGCN, a novel SNE approach that learns node embeddings based on the trustworthiness on edge signs. We first formulate the problem of SNE and present an overview of TrustSGCN. The SNE problem is formulated as follows. Let $\mathcal{G} = (\mathcal{V}, \mathcal{E}^+, \mathcal{E}^-)$ be a given signed network, where $\mathcal{V} = \{v_1, v_2, \dots, v_l\}$ denotes the set of l nodes, and \mathcal{E}^+ and \mathcal{E}^- represent the sets of positive and negative edges, respectively. SNE methods aim to learn a function $\mathbf{f}: \mathcal{V} \rightarrow \mathbb{R}^d$, which maps each node $v_i \in \mathcal{V}$ to a d -dimensional embedding.

TrustSGCN generates the node embeddings via three key modules (see Figure 3): (M1) generation of extended ego networks (EgoNets), (M2) measurement of trustworthiness on edge signs, and (M3) trustworthiness-aware propagation of embeddings. Then, TrustSGCN learns them through a loss function based on the balance and status theories. Table II summarizes a list of notations used in this paper.

A. Key Modules

For each node v_i in a given signed network \mathcal{G} , TrustSGCN randomly generates v_i ’s (initial) positive and negative

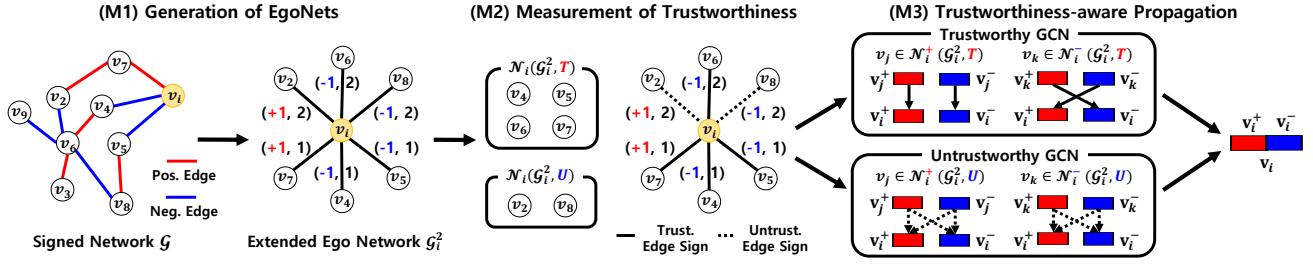


Fig. 3. Overview of TrustSGCN, which performs embedding propagation by considering trustworthiness on edge signs.

TABLE II
NOTATIONS USED IN THIS PAPER

Notation	Description
\mathcal{G}	Signed network
\mathcal{V}	Set of nodes
$\mathcal{E}, \mathcal{E}^+, \mathcal{E}^-$	Sets of edges, positive edges, and negative edges
$\mathbf{v}_i, \mathbf{v}_i^+, \mathbf{v}_i^-$	Embedding, positive embedding, negative embedding of v_i
$\mathbf{m}^+, \mathbf{m}^-$	Positive and negative message
d	Dimensionality of embeddings
\mathcal{G}_i^n	v_i 's EgoNet with neighbors of v_i whose path lengths from v_i are less than or equal to n in \mathcal{G}
$\mathcal{N}_i^n(\mathcal{G})$	Set of v_i 's neighbors whose path lengths from v_i are less than or equal to n in \mathcal{G}
$e_{ij} = (s_{ij}, p_{ij})$	Label for each edge in \mathcal{G}_i^n , including a pair of an edge sign s_{ij} and a path length p_{ij}
$\hat{s}_{ij}, Trust(\hat{s}_{ij})$	Edge sign between v_i and v_j and its trustworthiness inferred by FExtra
$\mathcal{N}_i^+(G_i^n, T), \mathcal{N}_i^-(G_i^n, U)$	Sets of v_i 's neighbors with trustworthy and untrustworthy edge signs in \mathcal{G}_i^n
$\mathcal{N}_i^+(G_i^n, *), \mathcal{N}_i^-(G_i^n, *)$	Sets of v_i 's neighbors with $s_{ij} = +1$ and $s_{ij} = -1$ in \mathcal{G}_i^n
H	Number of T-GCN and U-GCN layers
$r_{(a,b,c)}$	Ratio of propagation according to two prior signs (<i>i.e.</i> , a and b) and a posterior sign (<i>i.e.</i> , c)
n	Maximum path length between two nodes to be included in the EgoNet
$\alpha_{p_{ij}}$	Attention weight according to p_{ij}
β	Pre-defined threshold for $Trust(\hat{s}_{ij})$
γ	Number of randomly sampled nodes
λ	Weight for the status loss

embeddings $\mathbf{v}_i^+, \mathbf{v}_i^-$ and performs the following three modules sequentially.

(M1) Generation of EgoNets. We sample a set of nodes v_j among v_i 's indirect neighbors in \mathcal{G} , where the trustworthiness on the edge signs between v_i and v_j predicted by balance theory will be measured (*i.e.*, M2) and the trustworthiness-based propagation will be conducted (*i.e.*, M3). To this end, we generate v_i 's EgoNet consisting of edges between v_i and v_j (*i.e.*, v_i 's direct and n -hop neighbors in \mathcal{G}). The intuition behind this design choice is that since the prediction accuracy on edge signs by balance theory decreases rapidly as the length of the path between two nodes increases [16], we only use nodes v_j , whose paths from v_i are short, as v_i 's neighbors in EgoNet. That is, a v_i 's EgoNet \mathcal{G}_i^n can be defined:

$$\mathcal{G}_i^n = \{(v_i, e_{ij}, v_j) | v_j \in \mathcal{N}_i^n(\mathcal{G}), e_{ij} = (s_{ij}, p_{ij})\}, \quad (1)$$

where $\mathcal{N}_i^n(\mathcal{G})$ represents a set of nodes v_j whose path length from v_i is less than or equal to n in \mathcal{G} ; also, e_{ij} indicates an edge label between v_i and v_j , including a pair of an edge sign $s_{ij} \in \{+1, -1\}$ and a path length p_{ij} . Here, for s_{ij} between v_i and its indirect neighbors v_j in \mathcal{G} , we assign the edge signs predicted by the balance theory.

For instance, consider v_2 and v_6 in Figure 3, which are 2-hop neighbors of v_i . In this case, we can consider v_2 (resp. v_6) as the friend (resp. enemy) of v_i based on the balance theory, since there exists an even (resp. odd) number of negative edges between v_2 (resp. v_6) and v_i . Consequently, the edge signs s_{i2} and s_{i6} in \mathcal{G}_i^n are assigned positive and negative, respectively. Moreover, when there are multiple paths from v_i to v_j in \mathcal{G} with lengths less than or equal to n , the EgoNet \mathcal{G}_i^n of v_i takes the form of a *multigraph* [38], [39], which allows multiple edges between the same pair of nodes. However, note that if there is a direct edge between v_i and v_j , longer paths are discarded. The intuition behind this is to avoid the noise arising from uncertain high-order relationships when we have a *reliable* direct edge.

Suppose that we construct v_i 's EgoNet \mathcal{G}_i^3 by using its 3-hop neighbors (*i.e.*, $n = 3$). In this scenario, there are three distinct paths between v_i and v_6 in Figure 3, *i.e.*, (v_i, v_4, v_6) , (v_i, v_7, v_2, v_6) , and (v_i, v_5, v_8, v_6) . As a result, \mathcal{G}_i^3 includes three edges between v_i and v_6 . Since these edges may have different labels, one can raise concerns about the cases where the same pair of nodes exhibit both positive and negative signs through different paths. However, TrustSGCN can address such a contradictory case by not only measuring the trustworthiness of each edge sign in (M2) but also prioritizing more frequent propagation of the majority sign in (M3).

(M2) Measurement of Trustworthiness on Edge Signs.

We measure the trustworthiness on the edge signs s_{ij} in \mathcal{G}_i^n generated by (M1). Note that \mathcal{G}_i^n includes both *existent* and *non-existent* edges in the input signed network \mathcal{G} : the existent edges have *actual signs* expressed in \mathcal{G} , while the non-existent edges have *inferred signs* by balance theory. In this sense, we assume that the actual signs are all trustworthy. On the other hand, since the balance theory usually provides inaccurate predictions on edge signs (see Table I), we measure the trustworthiness on the inferred signs.

Accordingly, for the edges with $p_{ij} \geq 2$ in \mathcal{G}_i^n , we predict their signs in a different way by utilizing the additional *topological information* related to both v_i and v_j (not the combination of the edge signs included in the path from v_i to v_j). Specifically, we first learn a logistic regression classifier model, FExtra [40], [41], based on various topological features. To this end, we first extract 23 features for each node pair (v_i, v_j) in \mathcal{G} , thus constructing a feature vector $\mathbf{f}_{i,j} = \{f_1(i, j), \dots, f_{23}(i, j)\}$ for the corresponding node pair, where $f_k(i, j)$ indicates k -th feature value for the node pair. Among the 23 features, 7 features are related to the degrees of v_i and v_j . On the other hand, the remaining 16 features are related to the triads consisting of v_i, v_j , and

their common neighbors in \mathcal{G} . The details for features can be founded in Appendix A.

Using the learned classifier, we then predict the sign, $\hat{s}_{ij} \in \{+1, -1\}$, of each edge with $p_{ij} \geq 2$ in \mathcal{G}_i^n (i.e., non-existent edge in \mathcal{G}) based on the following probabilities:

$$\begin{aligned} P(+|\mathbf{f}_{i,j}) &= \frac{1}{1 + e^{-(b_0 + \sum_{k=1}^{23} b_k f_k(i,j))}}, \\ P(-|\mathbf{f}_{i,j}) &= 1 - P(+|\mathbf{f}_{i,j}), \end{aligned} \quad (2)$$

where $P(+|\mathbf{f}_{i,j})$ and $P(-|\mathbf{f}_{i,j})$ represent the probability that the edge sign between v_i and v_j is positive and negative, respectively. Also, b_0 indicates a bias coefficient, and b_1, \dots, b_{23} indicate coefficients for each feature, all of which are estimated based on training data [40], [41]. Meanwhile, the classifier also outputs the trustworthiness, $Trust(\hat{s}_{ij})$, on the inferred edge sign \hat{s}_{ij} . Note that we perform this sign prediction task as a pre-processing task in advance to avoid the computational overhead for the training of TrustSGCN.

Based on \hat{s}_{ij} and $Trust(\hat{s}_{ij})$, we now decide whether each edge sign s_{ij} predicted by balance theory is trustworthy or not. To this end, we employ the following two conditions [16]:

- (C1) $Trust(\hat{s}_{ij}) > \beta$, where β represents a pre-defined threshold for $Trust(\hat{s}_{ij})$
- (C2) $\hat{s}_{ij} = s_{ij}$

That is, we consider s_{ij} predicted by balance theory as trustworthy if both conditions are satisfied, otherwise untrustworthy. In other words, when $Trust(\hat{s}_{ij})$ gets higher than a pre-defined threshold and the edge signs predicted by FExtra and by balance theory are identical, we finally trust s_{ij} predicted by balance theory. By doing so, we can classify v_i 's neighbors v_j in \mathcal{G}_i^n into two subsets: a set $\mathcal{N}_i^+(\mathcal{G}_i^n, T)$ of v_j with *trustworthy* edge signs and another set $\mathcal{N}_i^-(\mathcal{G}_i^n, U)$ of v_j with *untrustworthy* edge signs. Also, each subset can be divided according to the edge signs s_{ij} , i.e., $\mathcal{N}_i^+(\mathcal{G}_i^n, *)$ and $\mathcal{N}_i^-(\mathcal{G}_i^n, *)$.

(M3) Trustworthiness-aware Propagation of Embeddings.

We perform different embedding propagation according to the subsets obtained from (M2). To this end, we devise two types of GCN: (1) trustworthy GCN (in short, T-GCN) propagates the embeddings of nodes in $\mathcal{N}_i^+(\mathcal{G}_i^n, T)$ to v_i ; (2) untrustworthy GCN (in short, U-GCN) propagates the embeddings of nodes in $\mathcal{N}_i^-(\mathcal{G}_i^n, U)$ to v_i .

Specifically, T-GCN generates positive and negative messages, $\mathbf{m}_{i \leftarrow T}^+(h)$ and $\mathbf{m}_{i \leftarrow T}^-(h)$, of nodes $v_j \in \mathcal{N}_i^+(\mathcal{G}_i^n, T)$ and $v_k \in \mathcal{N}_i^-(\mathcal{G}_i^n, T)$ with trustworthy edge signs, which will be propagated to v_i :

$$\begin{aligned} \mathbf{m}_{i \leftarrow T}^+(h) &= \sigma \left(\mathbf{w}^+(h) \left(\sum_{v_j \in \mathcal{N}_i^+(\mathcal{G}_i^n, T)} \alpha_{p_{ij}} \mathbf{v}_j^+(h-1) \right. \right. \\ &\quad \left. \left. + \sum_{v_k \in \mathcal{N}_i^-(\mathcal{G}_i^n, T)} \alpha_{p_{ik}} \mathbf{v}_k^-(h-1) \right) \right), \\ \mathbf{m}_{i \leftarrow T}^-(h) &= \sigma \left(\mathbf{w}^-(h) \left(\sum_{v_j \in \mathcal{N}_i^+(\mathcal{G}_i^n, T)} \alpha_{p_{ij}} \mathbf{v}_j^-(h-1) \right. \right. \\ &\quad \left. \left. + \sum_{v_k \in \mathcal{N}_i^-(\mathcal{G}_i^n, T)} \alpha_{p_{ik}} \mathbf{v}_k^+(h-1) \right) \right), \end{aligned} \quad (3)$$

where $\hat{\mathcal{N}}_i^+(\mathcal{G}_i^n, T)$ and $\hat{\mathcal{N}}_i^-(\mathcal{G}_i^n, T)$ represent sets of randomly sampled γ nodes from $\mathcal{N}_i^+(\mathcal{G}_i^n, T)$ and $\mathcal{N}_i^-(\mathcal{G}_i^n, T)$,

respectively. Note that random sampling is performed for each node v_i to achieve efficient learning [42] and mitigate the issues of over-smoothing [43] and over-fitting [44], which will be validated in Section IV-B. Additionally, $\mathbf{v}_j^+(h-1)$ and $\mathbf{v}_j^-(h-1)$ denote the positive and negative embeddings of node v_j from the $(h-1)$ -th layer, respectively. Also, σ indicates a sigmoid function, and $\mathbf{W}^+(h)$ and $\mathbf{W}^-(h)$ represent the learnable weight matrices of the h -th layer. Furthermore, $\alpha_{p_{ij}}$ represents the learnable attention, controlling the weight of propagation for v_j 's embeddings according to the path length p_{ij} from v_i to v_j . Intuitively, T-GCN propagates the embeddings of the *same* polarity from $v_j \in \hat{\mathcal{N}}_i^+(\mathcal{G}_i^n, T)$ to v_i , while propagating the embeddings of the *opposite* polarity from $v_k \in \hat{\mathcal{N}}_i^-(\mathcal{G}_i^n, T)$ to v_i , in the same way as in the existing GCN-based SNE methods [23], [25].

Next, U-GCN generates positive and negative messages, $\mathbf{m}_{i \leftarrow U}^+(h)$ and $\mathbf{m}_{i \leftarrow U}^-(h)$, of nodes $v_j \in \mathcal{N}_i^+(\mathcal{G}_i^n, U)$ and $v_k \in \mathcal{N}_i^-(\mathcal{G}_i^n, U)$ with untrustworthy edge signs, which will be propagated to v_i :

$$\begin{aligned} \mathbf{m}_{i \leftarrow U}^+(h) &= \sigma \left(\mathbf{w}^+(h) \left(\sum_{v_j \in \hat{\mathcal{N}}_i^+(\mathcal{G}_i^n, U)} \alpha_{p_{ij}} \left(r_{(+++)} \mathbf{v}_j^+(h-1) + r_{(-++)} \mathbf{v}_j^-(h-1) \right) \right. \right. \\ &\quad \left. \left. + \sum_{v_k \in \hat{\mathcal{N}}_i^-(\mathcal{G}_i^n, U)} \alpha_{p_{ik}} \left(r_{(+-+)} \mathbf{v}_k^+(h-1) + r_{(---)} \mathbf{v}_k^-(h-1) \right) \right) \right), \\ \mathbf{m}_{i \leftarrow U}^-(h) &= \sigma \left(\mathbf{w}^-(h) \left(\sum_{v_j \in \hat{\mathcal{N}}_i^+(\mathcal{G}_i^n, U)} \alpha_{p_{ij}} \left(r_{(+-+)} \mathbf{v}_j^+(h-1) + r_{(-+-)} \mathbf{v}_j^-(h-1) \right) \right. \right. \\ &\quad \left. \left. + \sum_{v_k \in \hat{\mathcal{N}}_i^-(\mathcal{G}_i^n, U)} \alpha_{p_{ik}} \left(r_{(+-+)} \mathbf{v}_k^+(h-1) + r_{(---)} \mathbf{v}_k^-(h-1) \right) \right) \right), \end{aligned} \quad (4)$$

where $r_{(a,b,c)}$ represents the ratio at which v_j 's or v_k 's signed embeddings are partially propagated to v_i according to the following three signs: (1) \mathbf{v}_j^a or \mathbf{v}_k^a (i.e., a sign a of v_j 's or v_k 's embedding to be propagated); (2) $\mathcal{N}_i^b(\mathcal{G}_i^n, U)$ (i.e., a sign b of the subset that includes v_j or v_k); and (3) $\mathbf{m}_{i \leftarrow U}^c(h)$ (i.e., a sign c of the message propagated to v_i). For determining ratios of propagation, we consider the structural properties inherent to the input network \mathcal{G} . Specifically, given two prior signs a and b , we leverage the ratio of triads with a posterior sign c in \mathcal{G} (see Table I). For example, when the input network \mathcal{G} is Epinions, $r_{(+-+)}$ and $r_{(+--)}$ become 0.71 and 0.29, respectively. The intuition behind this design choice is that since the edge sign between the two nodes v_i and $v_j \in \hat{\mathcal{N}}_i^+(\mathcal{G}_i^n, U)$ (resp. $v_k \in \hat{\mathcal{N}}_i^-(\mathcal{G}_i^n, U)$) is uncertain, both positive and negative embeddings of v_j (resp. v_k) are partially included in both positive and negative messages [16]. By doing so, we can correct the incorrect propagation by referring to the statistics of a given network without the need for hyperparameters.

Figure 4 illustrates the cases where the positive and negative messages of v_i are generated by U-GCN on the Epinions dataset. The cases are divided into four groups according to two prior signs a, b for two nodes v_i and v_j/v_k . When the inferred edge sign s_{ij} is positive (i.e., $b = +$), U-GCN propagates 96% (i.e., $r_{(+++)}$) and 4% (i.e., $r_{(+-+)}$) of v_j 's

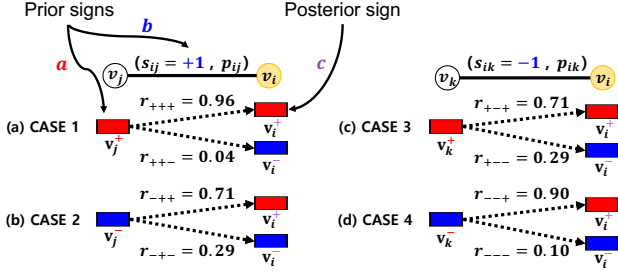


Fig. 4. Embedding propagation of untrustworthy GCN on Epinions.

positive embedding \mathbf{v}_j^+ to v_i 's positive and negative embeddings \mathbf{v}_i^+ and \mathbf{v}_i^- , respectively (*i.e.*, CASE 1). Also, it propagates 71% (*i.e.*, $r_{(---)}$) and 29% (*i.e.*, $r_{(-++)}$) of v_j 's negative embedding \mathbf{v}_j^- to \mathbf{v}_i^+ and \mathbf{v}_i^- , respectively (*i.e.*, CASE 2). On the other hand, when the inferred edge sign s_{ik} is negative (*i.e.*, $b = -$), U-GCN propagates 71% (*i.e.*, $r_{(---)}$) and 29% (*i.e.*, $r_{(+--)}$) of v_k 's positive embedding \mathbf{v}_k^+ to \mathbf{v}_i^+ and \mathbf{v}_i^- , respectively (*i.e.*, CASE 3). Also, it propagates 90% (*i.e.*, $r_{(-++)}$) and 10% (*i.e.*, $r_{(---)}$) of v_k 's negative embedding \mathbf{v}_k^- to \mathbf{v}_i^+ and \mathbf{v}_i^- , respectively (*i.e.*, CASE 4). It should be noted that TrustSGCN pre-computes the statistics regarding triads for a given signed network as part of a pre-processing task.

Now, TrustSGCN updates positive and negative embeddings, $\mathbf{v}_i^+(h)$ and $\mathbf{v}_i^-(h)$, of v_i using the above signed messages as follows:

$$\begin{aligned} \mathbf{v}_i^+(h) &= \mathbf{v}_i^+(h-1) + \frac{1}{d_i^+} \left(\mathbf{m}_{i \leftarrow T}^+(h) + \mathbf{m}_{i \leftarrow U}^+(h) \right), \\ \mathbf{v}_i^-(h) &= \mathbf{v}_i^-(h-1) + \frac{1}{d_i^-} \left(\mathbf{m}_{i \leftarrow T}^-(h) + \mathbf{m}_{i \leftarrow U}^-(h) \right), \end{aligned} \quad (5)$$

where d_i^+ and d_i^- represent the numbers of nodes in $\hat{\mathcal{N}}_i^+(\mathcal{G}_i^n, *)$ and $\hat{\mathcal{N}}_i^-(\mathcal{G}_i^n, *)$, respectively. TrustSGCN considers v_i 's signed embeddings $\mathbf{v}_i^+(H)$ and $\mathbf{v}_i^-(H)$ obtained from the last H -th layer as v_i 's final signed embeddings \mathbf{v}_i^+ and \mathbf{v}_i^- . Finally, it fuses both signed embeddings into a single embedding \mathbf{v}_i , *i.e.*, $\mathbf{v}_i = \mathbf{v}_i^+ \parallel \mathbf{v}_i^-$.

B. Training

Given a directed edge (v_i, v_j) from v_i to v_j in the given signed network \mathcal{G} , TrustSGCN learns the embeddings of both nodes by employing two types of loss functions \mathcal{L}_{sign} and \mathcal{L}_{status} . These loss functions are designed based on social theories, working together to preserve the inherent properties (*i.e.*, sign and direction) of the edge in the embedding space.

First, \mathcal{L}_{sign} aims to learn edge signs based on the balance theory and is formulated as follows [24], [26], [27]:

$$\mathcal{L}_{sign} = \sum_{(v_i, v_j) \in \mathcal{E}} -y_{ij} \log(\sigma(\mathbf{v}_i \mathbf{v}_j)) - (1 - y_{ij}) \log(1 - \sigma(\mathbf{v}_i \mathbf{v}_j)), \quad (6)$$

where y_{ij} is 1 if the edge sign is positive, and 0 otherwise. Intuitively, the goal of this loss is to encourage high proximity between two nodes incident to a positive edge and low proximity between two nodes incident to a negative edge in the embedding space. By optimizing this objective, TrustSGCN naturally improves the preservation of the ternary relationships among the three nodes within balanced triads [10], [25].

TABLE III
DATASET STATISTICS

Datasets	Nodes	Edges	Positive Edges	Negative Edges
Bitcoin-Alpha	3,784	14,145	12,729 (89.9%)	1,416 (10.1%)
Bitcoin-OTC	5,901	21,522	18,390 (85.4%)	3,132 (14.6%)
Slashdot	13,182	36,338	30,914 (85.1%)	5,424 (14.9%)
Epinions	25,148	105,061	74,060 (70.5%)	31,001 (29.5%)

Second, \mathcal{L}_{status} aims to learn edge directions based on the status theory and is formulated as follows [26]:

$$\begin{aligned} \mathcal{L}_{status} = \sum_{(v_i, v_j) \in \mathcal{E}} & -y_{ij} \log \left(\sigma(s(\mathbf{v}_j) - s(\mathbf{v}_i)) \right) \\ & - (1 - y_{ij}) \log \left(\sigma(s(\mathbf{v}_i) - s(\mathbf{v}_j)) \right), \end{aligned} \quad (7)$$

where $s(\mathbf{v}_i) = \sigma(\mathbf{W} \cdot \mathbf{v}_i + \mathbf{b})$ indicates the status score of v_i , and \mathbf{W} and \mathbf{b} represent a learnable weight matrix and a bias term, respectively. Intuitively, guided by the status theory, the goal of this loss is to ensure that, for a positive edge, the destination node's status is higher than that of the source node, while for a negative edge, the destination node's status is lower than that of the source node.

By jointly optimizing the two losses above, the final loss function of TrustSGCN is defined as follows:

$$\mathcal{L} = \mathcal{L}_{sign} + \lambda \mathcal{L}_{status}, \quad (8)$$

where λ indicates a weight parameter for the status loss. We will analyze the sensitivity of TrustSGCN to λ in Section IV-B.

IV. EVALUATION

We designed our experiments, aiming at answering the following key evaluation questions (EQs):

- (EQ1) Does trustworthiness-aware propagation yield effective results for a sign prediction task?
- (EQ2) Does joint learning of two types of loss functions yield effective results for a sign prediction task?
- (EQ3) Does TrustSGCN achieve superior performance compared to its competitors for a sign prediction task?
- (EQ4) How do different values of a parameter β in TrustSGCN influence the sign prediction accuracy?
- (EQ5) How is the computational overhead (*i.e.*, training time) of TrustSGCN compared with its competitors?

A. Experimental Setup

Datasets. We used four real-world signed network datasets, which are widely used in previous studies of SNE [23]–[27]: Bitcoin-Alpha, Bitcoin-OTC, Slashdot, and Epinions. The datasets are all publicly available.² Table III provides some statistics for the four datasets.

Competitors. We compared TrustSGCN with five state-of-the-art GCN-based SNE methods: SGCN [23], SiGAT [24], SNEA [25], SDGNN [26], and SGCL [27]. For a fair comparison, we set the dimensionality of embeddings to 64 in all methods, following [23], [25].

Evaluation Task. For testing, we split a dataset into training (80%) and test (20%) sets. Following [23]–[27], we employ

²<https://snap.stanford.edu/data>, <https://www.aminer.cn/data-sna>

TABLE IV
SIGN PREDICTION ACCURACIES OF TRUSTSGCN, TRUSTSGCN(T-GCN), AND TRUSTSGCN(FEXTRA)

Datasets Metrics	Bitcoin-Alpha			Bitcoin-OTC			Slashdot			Epinions		
	Micro-F1	Macro-F1	AUC	Micro-F1	Macro-F1	AUC	Micro-F1	Macro-F1	AUC	Micro-F1	Macro-F1	AUC
TrustSGCN	0.921	0.721	0.867	0.901	0.773	0.886	0.891	0.765	0.907	0.920	0.902	0.966
TrustSGCN(T-GCN)	0.914	0.708	0.852	0.895	0.761	0.880	0.885	0.735	0.904	0.916	0.897	0.965
TrustSGCN(FEXtra)	0.913	0.697	0.850	0.891	0.745	0.880	0.889	0.754	0.903	0.912	0.892	0.961

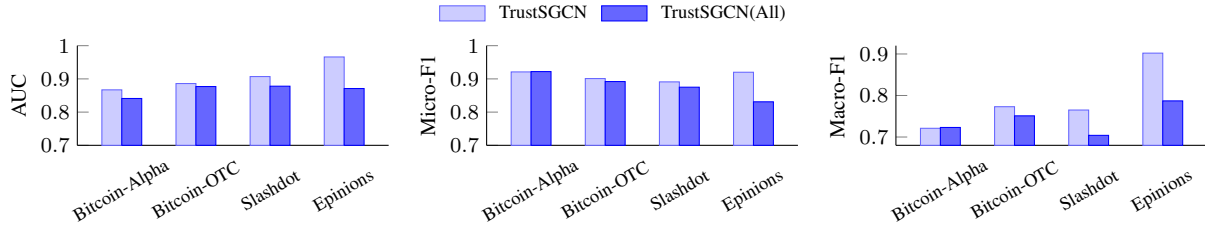


Fig. 5. Sign prediction accuracies of TrustSGCN and TrustSGCN(All).

an edge sign prediction task, which aims to evaluate how accurately each SNE method classifies the edge signs. To measure the accuracy, we use the three popular metrics: F1-Micro, F1-Macro, and *area under curve* (AUC) [45].

Implementation Details. All the experiments were conducted on NVIDIA TITAN Xp GPUs with 12GB memory. We carefully tuned the hyperparameters of competitors and TrustSGCN. For hyperparameters of competitors, we used the best settings found via grid search. For TrustSGCN, we consistently set $n = 3$ (*i.e.*, the number of hops) and $H = 1$ (*i.e.*, the number of GCN layers) for all datasets. In addition, for Bitcoin-Alpha, Bitcoin-OTC, Slashdot, and Epinions, we set γ (*i.e.*, the number of randomly sampled nodes) to 30, 30, 20, and 10, β (*i.e.*, a pre-defined threshold for $Trust(\hat{s}_{ij})$) to 0.80, 0.95, 1, and 1, and λ (*i.e.*, a weight parameter for the status loss) to 1, 0.80, 1, and 1, respectively.

B. Results and Analysis

In this section, we omit some experimental results when we confirmed that the performance of TrustSGCN for other metrics or parameter settings is consistent with that of the reported results. The details for the omitted results are available in Appendix B.

Results for EQ1. To validate the effectiveness of our key ideas regarding trustworthiness-aware propagation, we conducted experiments to answer the following four sub-questions:

- **EQ1-1 (Trustworthiness Awareness):** Does considering the trustworthiness for high-order signed relationships, inferred by balance theory, help to improve sign prediction accuracies?
- **EQ1-2 (Random Sampling):** Does the random sampling of each node’s neighbors, used for embedding propagation, help to improve sign prediction accuracies?
- **EQ1-3 (Propagation Ratios):** Does incorporating the statistics of a given network for untrustworthy edge signs help to improve sign prediction accuracies?

- **EQ1-4 (Path-length-based Attention):** Does using learnable attention to control the propagation weight based on a path length help to improve sign prediction accuracies?

For EQ1-1, we use two variants of TrustSGCN that do not employ U-GCN: (1) TrustSGCN(T-GCN), which performs embedding propagation based on the edge signs predicted by balance theory (*i.e.*, using only T-GCN); and (2) TrustSGCN(FEXtra), which performs embedding propagation based on the edge signs predicted by FEXtra, instead of balance theory. Table IV demonstrates that TrustSGCN consistently outperforms both variants across all datasets. We observed that the ratio of neighbors with untrustworthy edge signs, among all the neighbors in each node’s EgoNet, exceeds 45% on all datasets. This finding suggests that the predictions made by balance theory or FEXtra are often incorrect, and correcting these incorrect predictions is beneficial to sign predictions more accurate.

For EQ1-2, we use a variant of TrustSGCN, called TrustSGCN(All), which uses all of each node’s neighbors (without random sampling) during embedding propagation. Figure 5 illustrates that TrustSGCN outperforms TrustSGCN(All) across all datasets in almost all cases. Notably, we observed that this sampling strategy is significantly effective for large datasets such as Slashdot and Epinions. The results can be attributed to the mitigation of the over-fitting and over-smoothing problems achieved by random sampling, which is consistent with the findings reported in previous studies [43], [44].

For EQ1-3, we use two variants of TrustSGCN that employ different propagation ratios in U-GCN: (1) TrustSGCN(Uniform), which *uniformly* propagates to both positive and negative embeddings with an equal ratio (*i.e.*, 50:50); and (2) TrustSGCN(Reverse), which *differently* propagates to positive and negative embeddings using the inverse of the ratios used in our U-GCN. Table V illustrates that TrustSGCN consistently and significantly outperforms both variants. The results demonstrate that leveraging the intrinsic properties of the input network is the most effective approach to avoid incorrect propagation when propagating to signed embeddings.

TABLE V
SIGN PREDICTION ACCURACIES OF TRUSTSGCN, TRUSTSGCN(UNIFORM), TRUSTSGCN(REVERSE), AND TRUSTSGCN(MEAN)

Datasets Metrics	Bitcoin-Alpha			Bitcoin-OTC			Slashdot			Epinions		
	Micro-F1	Macro-F1	AUC	Micro-F1	Macro-F1	AUC	Micro-F1	Macro-F1	AUC	Micro-F1	Macro-F1	AUC
TrustSGCN	0.921	0.721	0.867	0.901	0.773	0.886	0.891	0.765	0.907	0.920	0.902	0.966
TrustSGCN(Uniform)	0.918	0.710	0.860	0.896	0.762	0.873	0.884	0.753	0.900	0.917	0.898	0.964
TrustSGCN(Reverse)	0.912	0.700	0.841	0.894	0.752	0.881	0.887	0.750	0.904	0.915	0.895	0.964
TrustSGCN(Mean)	0.919	0.716	0.855	0.899	0.771	0.882	0.883	0.734	0.901	0.914	0.894	0.964

TABLE VI
THE EFFECT OF λ ON SIGN PREDICTION ACCURACIES OF TRUSTSGCN

Datasets	Metrics	$\lambda=0$	$\lambda=0.2$	$\lambda=0.4$	$\lambda=0.6$	$\lambda=0.8$	$\lambda=1$
Bitcoin-Alpha	Micro-F1	0.917	0.912	0.917	0.920	0.916	0.921
	Macro-F1	0.705	0.698	0.705	0.723	0.700	0.721
	AUC	0.861	0.859	0.861	0.865	0.861	0.867
Bitcoin-OTC	Micro-F1	0.895	0.899	0.895	0.896	0.901	0.898
	Macro-F1	0.762	0.772	0.762	0.762	0.773	0.770
	AUC	0.881	0.883	0.881	0.882	0.886	0.881
Slashdot	Micro-F1	0.889	0.890	0.885	0.881	0.888	0.891
	Macro-F1	0.750	0.756	0.751	0.743	0.750	0.765
	AUC	0.904	0.905	0.904	0.901	0.905	0.907
Epinions	Micro-F1	0.910	0.911	0.911	0.912	0.911	0.919
	Macro-F1	0.890	0.891	0.890	0.892	0.890	0.901
	AUC	0.960	0.961	0.962	0.963	0.964	0.966

For EQ1-4, we use a variant of TrustSGCN, called TrustSGCN(Mean), which uses mean pooling instead of an attention mechanism during embedding propagation. Table V indicates that using the attention mechanism yields higher sign prediction accuracy compared to mean pooling. It demonstrates the significance of assigning different weights to nodes during embedding propagation based on their path lengths.

Results for EQ2. To evaluate the effectiveness of the joint learning of \mathcal{L}_{sign} and \mathcal{L}_{status} , we investigate the impact of the weight parameter λ for the status loss on the sign prediction performance of TrustSGCN. Table VI presents the results. It demonstrates that the accuracy of TrustSGCN is the lowest when $\lambda=0$, while it is the highest when $\lambda=1$ in almost all cases. The results emphasize the importance of simultaneously learning both the sign and direction information of the input network through L_{sign} and L_{status} .

Results for EQ3. We conducted comparative experiments on a sign prediction task to demonstrate the superiority of TrustSGCN over 5 state-of-the-art SNE methods. To do this, we use $x(=80, 60, 40, 20)\%$ of the existent edges in each dataset as the training set and the remaining edges as the test set. That is, as the value of x decreases, the sparsity of the training set increases. Table VII shows the results for AUC. The values boldfaced and underlined indicate the best and 2nd-best accuracies in each row (*i.e.*, each dataset), respectively.

We summarize the results shown in Table VII as follows. First, among the competitors, no single method consistently

outperforms the others. That is, the best competitors vary per dataset and training ratio. Second and most importantly, TrustSGCN universally outperforms *all* competitors in *all* settings on *all* datasets. Notably, we highlight that as the value of x decreases, the accuracy improvement of TrustSGCN over competitors tends to increase. Specifically, on Bitcoin-OTC, TrustSGCN yields up to 0.45% and 2.18% higher AUC than the best competitor (*i.e.*, SGCL and SDGNN) when x is 80 and 20, respectively. Moreover, on Slashdot, TrustSGCN yields up to 1.45% and 2.09% higher AUC than the best competitor (*i.e.*, SiGAT) when x is 80 and 20, respectively. The results show that considering the trustworthiness on edge signs is helpful in accurately preserving the proximities between nodes (in particular, when information on nodes is insufficient), which leads to improving the accuracy of the sign prediction task.

Results for EQ4. We analyze the change of the accuracy according to different values of β (*i.e.*, a threshold for $Trust(\hat{s}_{ij})$) in TrustSGCN. Figure 6 shows the results, where the x -axis and y -axis represent the values of β and AUCs, respectively. The optimal value of β that yields the highest accuracy varies across different datasets. Specifically, for Bitcoin-Alpha, Bitcoin-OTC, Slashdot, and Epinions, the highest accuracy is achieved when β is set to 0.80, 0.95, 1.00, and 1.00, respectively. Overall, to achieve higher accuracy in the sign prediction task, it is crucial to set β to a relatively higher value. This indicates that we should exploit the predicted edge signs only when the predictions by FExtra are sufficiently confident.

Results for EQ5. We conducted a comparison of the training times between TrustSGCN and its competitors. Figure 7 presents the results when we run a single epoch. The x -axis and the y -axis represent each method and the training time, respectively. We observe that, while TrustSGCN may not be the fastest method, its training time is still acceptable, especially when we consider the fact that TrustSGCN significantly and consistently outperforms the competitors in terms of accuracy. Therefore, we can conclude that TrustSGCN achieves higher accuracy than its competitors while requiring a reasonable training time.

V. CONCLUSIONS AND FUTURE WORK

In this work, we aimed to address the limitation of existing GCN-based SNE methods, which arise when relying blindly on the rules of balance theory. To overcome the limitation, we proposed a novel SNE method, named TrustSGCN, which learns node embeddings based on the trustworthiness on edge signs for signed graph convolutional networks. It consists of

TABLE VII
SIGN PREDICTION ACCURACIES OF 5 COMPETITORS AND TRUSTSGCN IN TERMS OF AUC

Training Ratios Methods	$x=80$						$x=60$					
	SGCN	SiGAT	SNEA	SDGNN	SGCL	TrustSGCN	SGCN	SiGAT	SNEA	SDGNN	SGCL	TrustSGCN
Bitcoin-Alpha	0.689	0.837	0.805	0.838	<u>0.840</u>	0.867	0.702	0.825	0.775	<u>0.835</u>	0.832	0.851
Bitcoin-OTC	0.763	0.875	0.805	0.876	<u>0.882</u>	0.886	0.740	0.871	0.796	0.870	<u>0.873</u>	0.887
Slashdot	0.805	<u>0.894</u>	0.788	0.876	0.858	0.907	0.791	<u>0.892</u>	0.791	0.871	0.843	0.907
Epinions	0.920	<u>0.961</u>	0.850	<u>0.961</u>	0.947	0.966	0.919	<u>0.954</u>	0.837	0.950	0.951	0.961

Training Ratios Methods	$x=40$						$x=20$					
	SGCN	SiGAT	SNEA	SDGNN	SGCL	TrustSGCN	SGCN	SiGAT	SNEA	SDGNN	SGCL	TrustSGCN
Bitcoin-Alpha	0.681	0.809	0.771	0.826	<u>0.827</u>	0.833	0.677	0.764	0.700	0.778	<u>0.781</u>	0.788
Bitcoin-OTC	0.732	<u>0.858</u>	0.804	0.854	0.852	0.875	0.672	0.819	0.746	<u>0.825</u>	0.798	0.843
Slashdot	0.773	<u>0.878</u>	0.779	0.870	0.852	0.895	0.777	<u>0.860</u>	0.763	0.853	0.837	0.878
Epinions	0.921	<u>0.948</u>	0.818	<u>0.948</u>	0.937	0.956	0.906	0.927	0.794	<u>0.940</u>	0.922	0.942

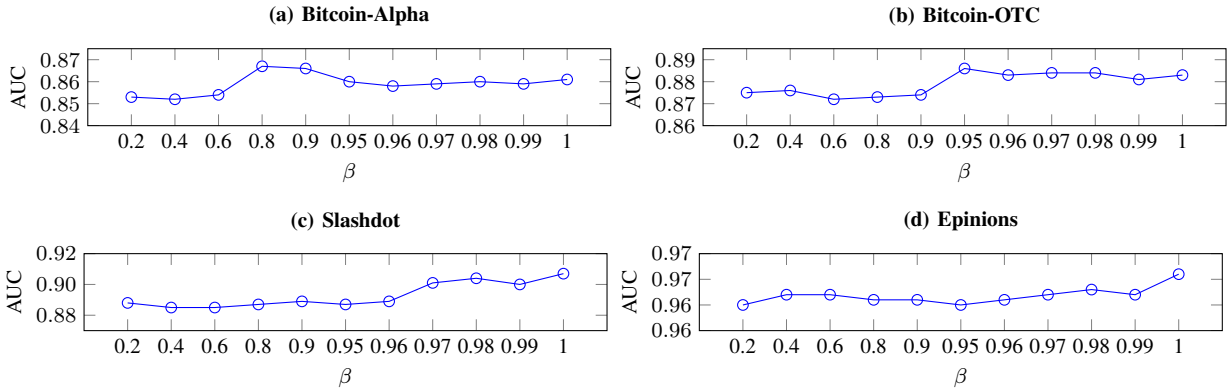


Fig. 6. The effect of β in a sign prediction task.

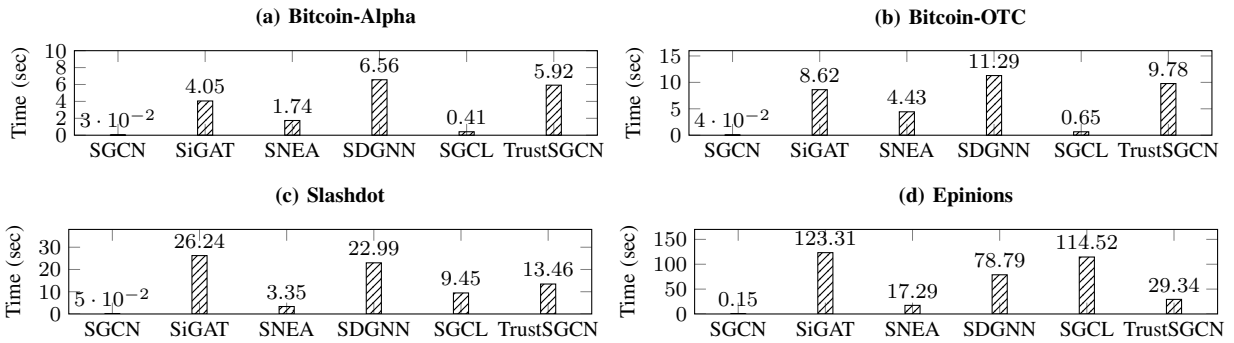


Fig. 7. Training times of 5 competitors and TrustSGCN.

the generation of EgoNets, the measurement of trustworthiness on edge signs, and the trustworthiness-aware propagation of embeddings. Additionally, we incorporated both balance and status theories into a loss function so that the sign and direction of edges can be preserved in the embedding space.

We conducted extensive experiments on four real-world signed network datasets to compare the performance of TrustSGCN with those of five existing GCN-based SNE methods. The results demonstrated that TrustSGCN consistently outperforms these methods in terms of sign prediction accuracy. We believe that our contribution is significant as we are the first to design a GCN architecture that explicitly considers the trustworthiness on edge signs. We hope that our work will encourage follow-up studies on trustworthy SNE research [46].

As future work, we plan to investigate an efficient way to reduce the computational time for preprocessing tasks such as FEXtra-based sign prediction and calculation of triad statistics. Furthermore, extending the applicability of TrustSGCN to other graph structures, such as multi-relational networks [47] or dynamic signed networks [48], would be an intriguing direction.

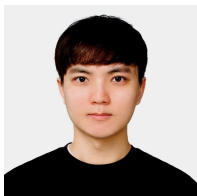
REFERENCES

- [1] J. Tang, Y. Chang, C. C. Aggarwal, and H. Liu, "A survey of signed network mining in social media," *ACM Computing Surveys*, vol. 49, no. 3, pp. 42:1–42:37, 2016.
- [2] S. Yuan, X. Wu, and Y. Xiang, "SNE: signed network embedding," in *Proceedings of Pacific-Asia Conference on Knowledge Discovery and Data Mining (PAKDD)*, 2017, pp. 183–195.

- [3] P. Doreian and A. Mrvar, "Structural balance and signed international relations," *Journal of Social Structure*, vol. 16, no. 1, p. 2, 2015.
- [4] T. Alsinet, J. Argelich, R. B ejjar, and S. Mart inez, "Measuring polarization in online debates," *Applied Sciences*, 2021.
- [5] O. Askarisichani, J. N. Lane, F. Bullo, N. E. Friedkin, A. K. Singh, and B. Uzzi, "Structural balance emerges and explains performance in risky decision-making," *Nature communications*, 2019.
- [6] F. Bonchi, E. Galimberti, A. Gionis, B. Ordozgoiti, and G. Ruffo, "Discovering polarized communities in signed networks," in *Proceedings of the ACM International Conference on Information and Knowledge Management (CIKM)*, 2019, pp. 961–970.
- [7] Y.-C. Lee, S.-W. Kim, and D. Lee, "goccf: Graph-theoretic one-class collaborative filtering based on uninteresting items," in *Proceedings of the AAAI Conference on Artificial Intelligence (AAAI)*, 2018.
- [8] W. Hwang, J. Parc, S. Kim, J. Lee, and D. Lee, "'told you i didn't like it': Exploiting uninteresting items for effective collaborative filtering," in *Proceedings of the IEEE International Conference on Data Engineering (ICDE)*, 2016, pp. 349–360.
- [9] Y. Ko, S. Ryu, S. Han, Y. Jeon, J. Kim, S. Park, K. Han, H. Tong, and S. Kim, "KHAN: knowledge-aware hierarchical attention networks for accurate political stance prediction," in *Proceedings of the ACM Web Conference 2023 (WWW)*. ACM, 2023, pp. 1572–1583.
- [10] S. Wang, J. Tang, C. C. Aggarwal, Y. Chang, and H. Liu, "Signed network embedding in social media," in *Proceedings of the SIAM International Conference on Data Mining (SDM)*, 2017, pp. 327–335.
- [11] Y. Lee, N. Seo, K. Han, and S. Kim, "Asine: Adversarial signed network embedding," in *Proceedings of the International ACM SIGIR Conference on Research and Development in Information Retrieval (SIGIR)*, 2020, pp. 609–618.
- [12] P. Xu, Y. Zhan, L. Liu, B. Yu, B. Du, J. Wu, and W. Hu, "Dual-branch density ratio estimation for signed network embedding," in *Proceedings of the ACM Web Conference (WWW)*, 2022, pp. 1651–1662.
- [13] Z. Huang, A. Silva, and A. K. Singh, "POLE: polarized embedding for signed networks," in *Proceedings of the ACM International Conference on Web Search and Data Mining (WSDM)*, 2022, pp. 390–400.
- [14] H. Yoo, Y. Lee, K. Shin, and S. Kim, "Directed network embedding with virtual negative edges," in *Proceedings of the ACM International Conference on Web Search and Data Mining (WSDM)*, 2022, pp. 1291–1299.
- [15] H. Wang, F. Zhang, M. Hou, X. Xie, M. Guo, and Q. Liu, "SHINE: signed heterogeneous information network embedding for sentiment link prediction," in *Proceedings of the ACM International Conference on Web Search and Data Mining (WSDM)*, 2018, pp. 592–600.
- [16] W. Lee, Y. Lee, D. Lee, and S. Kim, "Look before you leap: Confirming edge signs in random walk with restart for personalized node ranking in signed networks," in *Proceedings of the International ACM SIGIR Conference on Research and Development in Information Retrieval (SIGIR)*, 2021, pp. 143–152.
- [17] B. Hui, L. Zhang, X. Zhou, X. Wen, and Y. Nian, "Personalized recommendation system based on knowledge embedding and historical behavior," *Applied Intelligence*, vol. 52, no. 1, pp. 954–966, 2022.
- [18] J. Tang, C. C. Aggarwal, and H. Liu, "Recommendations in signed social networks," in *Proceedings of the ACM Web Conference (WWW)*, 2016, pp. 31–40.
- [19] T. Kim, J. Yu, W. Shin, H. Lee, J. Im, and S. Kim, "LATTE: A framework for learning item-features to make a domain-expert for effective conversational recommendation," in *Proceedings of the 29th ACM SIGKDD Conference on Knowledge Discovery and Data Mining (KDD)*. ACM, 2023, pp. 1144–1153.
- [20] M. Niepert, M. Ahmed, and K. Kutzkov, "Learning convolutional neural networks for graphs," in *Proceedings of the International Conference on Machine Learning (ICML)*, vol. 48, 2016, pp. 2014–2023.
- [21] T. N. Kipf and M. Welling, "Semi-supervised classification with graph convolutional networks," vol. abs/1609.02907, 2016.
- [22] Y.-C. Lee, J. Lee, D. Lee, and S.-W. Kim, "Thor: Self-supervised temporal knowledge graph embedding via three-tower graph convolutional networks," in *Proceedings of the IEEE International Conference on Data Mining (ICDM)*, 2022, pp. 1035–1040.
- [23] T. Derr, Y. Ma, and J. Tang, "Signed graph convolutional networks," in *Proceedings of the IEEE International Conference on Data Mining (ICDM)*, 2018, pp. 929–934.
- [24] J. Huang, H. Shen, L. Hou, and X. Cheng, "Signed graph attention networks," in *Proceedings of the International Conference on Artificial Neural Networks (ICANN)*, vol. 11731, 2019, pp. 566–577.
- [25] Y. Li, Y. Tian, J. Zhang, and Y. Chang, "Learning signed network embedding via graph attention," in *Proceedings of the AAAI Conference on Artificial Intelligence (AAAI)*, 2020, pp. 4772–4779.
- [26] J. Huang, H. Shen, L. Hou, and X. Cheng, "SDGNN: learning node representation for signed directed networks," in *Proceedings of the AAAI Conference on Artificial Intelligence (AAAI)*, 2021, pp. 196–203.
- [27] L. Shu, E. Du, Y. Chang, C. Chen, Z. Zheng, X. Xing, and S. Shen, "SGCL: contrastive representation learning for signed graphs," in *Proceedings of the ACM International Conference on Information and Knowledge Management (CIKM)*, 2021, pp. 1671–1680.
- [28] D. Cartwright and F. Harary, "Structural balance: a generalization of heider's theory," *Psychological Review*, vol. 63, no. 5, p. 277, 1956.
- [29] F. Heider, "Attitudes and cognitive organization," *The Journal of Psychology*, vol. 21, no. 1, pp. 107–112, 1946.
- [30] Y. Kang, W. Lee, Y.-C. Lee, K. Han, and S.-W. Kim, "Adversarial learning of balanced triangles for accurate community detection on signed networks," in *2021 IEEE International Conference on Data Mining (ICDM)*. IEEE, 2021, pp. 1150–1155.
- [31] E. Estrada, "Rethinking structural balance in signed social networks," *Discrete Applied Mathematics*, vol. 268, pp. 70–90, 2019.
- [32] J. Leskovec, D. Huttenlocher, and J. Kleinberg, "Signed networks in social media," in *Proceedings of the SIGCHI conference on human factors in computing systems*, 2010, pp. 1361–1370.
- [33] M. Kim, Y. Lee, and S. Kim, "Trustsgcn: Learning trustworthiness on edge signs for effective signed graph convolutional networks," in *Proceedings of the International ACM SIGIR Conference on Research and Development in Information Retrieval (SIGIR)*, 2023.
- [34] S. Wang, J. Tang, C. Aggarwal, Y. Chang, and H. Liu, "Signed network embedding in social media," in *Proceedings of the 2017 SIAM international conference on data mining*, 2017, pp. 327–335.
- [35] J. Kim, H. Park, J.-E. Lee, and U. Kang, "Side: representation learning in signed directed networks," in *Proceedings of the 2018 World Wide Web Conference*, 2018, pp. 509–518.
- [36] Y. Chen, T. Qian, H. Liu, and K. Sun, "'bridge' enhanced signed directed network embedding," in *Proceedings of International Conference on Information and Knowledge Management*, 2018, pp. 773–782.
- [37] H. Liu, "Lightsgcn: Powering signed graph convolution network for link sign prediction with simplified architecture design," in *Proceedings of the 45th International ACM SIGIR Conference on Research and Development in Information Retrieval*, 2022, pp. 2680–2685.
- [38] B. Boden, S. G unnemann, H. Hoffmann, and T. Seidl, "Mining coherent subgraphs in multi-layer graphs with edge labels," in *Proceedings of the ACM SIGKDD International Conference on Knowledge Discovery & Data Mining (KDD)*, 2012, pp. 1258–1266.
- [39] V. Ingalalli, D. Ienco, and P. Poncelet, "Mining frequent subgraphs in multigraphs," *Information Sciences*, vol. 451–452, pp. 50–66, 2018.
- [40] J. Leskovec, D. P. Huttenlocher, and J. M. Kleinberg, "Predicting positive and negative links in online social networks," in *Proceedings of the ACM Web Conference (WWW)*, 2010, pp. 641–650.
- [41] X. Li, H. Fang, and J. Zhang, "Rethinking the link prediction problem in signed social networks," in *Proceedings of the AAAI Conference on Artificial Intelligence (AAAI)*, 2017, pp. 4955–4956.
- [42] J. Chen, T. Ma, and C. Xiao, "Fastgcn: fast learning with graph convolutional networks via importance sampling," *arXiv preprint arXiv:1801.10247*, 2018.
- [43] W. Hamilton, Z. Ying, and J. Leskovec, "Inductive representation learning on large graphs," *Advances in neural information processing systems*, vol. 30, 2017.
- [44] T. N. Kipf and M. Welling, "Semi-supervised classification with graph convolutional networks," *arXiv preprint arXiv:1609.02907*, 2016.
- [45] J. A. Hanley and B. J. McNeil, "The meaning and use of the area under a receiver operating characteristic (roc) curve," *Radiology*, 1982.
- [46] H. Zhang, B. Wu, X. Yuan, S. Pan, H. Tong, and J. Pei, "Trustworthy graph neural networks: Aspects, methods and trends," *arXiv preprint arXiv:2205.07424*, 2022.
- [47] M.-H. Feng, C.-C. Hsu, C.-T. Li, M.-Y. Yeh, and S.-D. Lin, "Marine: Multi-relational network embeddings with relational proximity and node attributes," in *The World Wide Web Conference*, 2019, pp. 470–479.
- [48] Q.-V. Dang and C.-L. Ignat, "Link-sign prediction in dynamic signed directed networks," in *2018 IEEE 4th International Conference on Collaboration and Internet Computing (CIC)*, 2018, pp. 36–45.



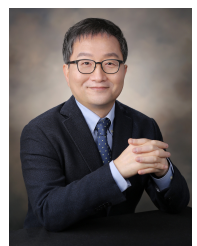
Min-Jeong Kim received the B.S. degree in Information and Communication Engineering from Chungbuk National University. She is currently a Ph.D. candidate in Artificial Intelligence at Hanyang University. Her research interests include graph mining, social network analysis, and recommender systems.



Yeon-Chang Lee received the Ph.D. degree in computer science from Hanyang University in 2021 and the B.S. degree in medical IT from Eulji university in 2014. He is currently a postdoctoral researcher at Georgia Institute of Technology. His research interests include recommender systems, graph mining, and graph representation learning.



David Y. Kang received the B.S. and Ph.D. degrees from Hanyang University in 2013 and 2022, respectively. He is currently a postdoctoral researcher at University of Michigan. His research interests include graph mining and social network analysis.



Sang-Wook Kim received the B.S. degree in computer engineering from Seoul National University, in 1989, and the M.S. and Ph.D. degrees in computer science from the Korea Advanced Institute of Science and Technology (KAIST), in 1991 and 1994, respectively. From 1995 to 2003, he served as an associate professor with Kangwon National University. In 2003, he joined Hanyang University, Seoul, Korea, where he currently is a professor in the Department of Computer Science and the director of the Brain-Korea-21-FOUR research program. He is

also leading a National Research Lab (NRL) Project funded by the National Research Foundation since 2015. From 2009 to 2010, he visited the Computer Science Department, Carnegie Mellon University, as a visiting professor. From 1999 to 2000, he worked with the IBM T. J. Watson Research Center, USA, as a postdoc. He also visited the Computer Science Department of Stanford University as a visiting researcher in 1991. He is an author of more than 200 papers in refereed international journals and international conference proceedings. His research interests include databases, data mining, multimedia information retrieval, social network analysis, recommendation, and web data analysis. He is a member of the ACM and the IEEE.

APPENDIX A

DETAILED DESCRIPTION OF TOPOLOGICAL FEATURES

We employed FExtra in (M2) to measure the trustworthiness of the edge signs predicted by the balance theory. FExtra serves as an additional approach capable of predicting high-order edge signs by leveraging the topological information associated with the two nodes. To this end, FExtra utilizes 23 features for each node pair (v_i, v_j) . Out of these 23 features, 7 features are related to the degrees of v_i and v_j (i.e., (f1) ~ (f7)), while the remaining 16 features are related to the triads consisting of v_i , v_j , and their common neighbors in \mathcal{G} (i.e., (f8) ~ (f23)):

- (f1): the number of v_i 's positive edges
- (f2): the number of v_j 's positive edges
- (f3): the number of v_i 's negative edges
- (f4): the number of v_j 's negative edges
- (f5): the total degrees of v_i
- (f6): the total degrees of v_j
- (f7): the total number of common neighbors of v_i and v_j
- (f8), (f9), (f10), and (f11): the numbers of triads when the edge signs between v_i and each common neighbor v_z and those between v_j and v_z are both positive
- (f12), (f13), (f14), and (f15): the numbers of triads when the edge signs between v_i and each common neighbor v_z and those between v_j and v_z are positive and negative, respectively
- (f16), (f17), (f18), and (f19): the numbers of triads when the edge signs between v_i and each common neighbor v_z and those between v_j and v_z are negative and positive, respectively
- (f20), (f21), (f22), and (f23): the numbers of triads when the edge signs between v_i and each common neighbor v_z and those between v_j and v_z are both negative

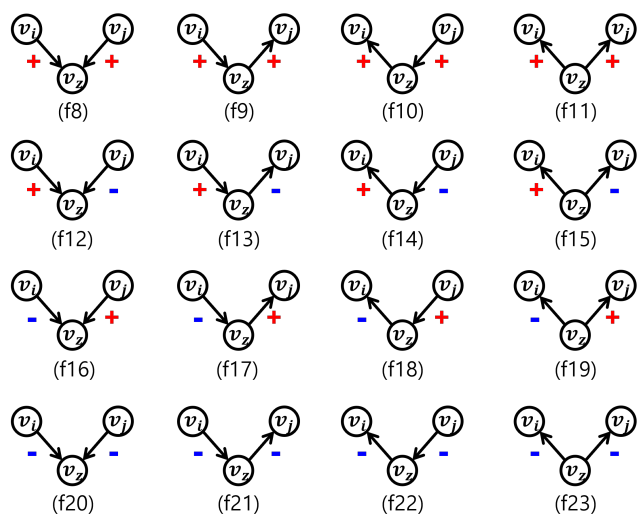


Fig. 8. 16 types of triads consisting of two nodes v_i , v_j and a common neighbor v_z .

For features (f8) to (f23), the distinction is made based on whether the direction of the two edges is outgoing or incoming, as depicted in Figure 8. In other words, they are

TABLE VIII
THE EFFECT OF γ ON SIGN PREDICTION ACCURACIES OF TRUSTSGCN WHEN WE SET x TO 80

Datasets	Metrics	$\gamma=10$	$\gamma=20$	$\gamma=30$	$\gamma=40$	$\gamma=50$	$\gamma=60$	All
Bitcoin-Alpha	Micro-F1	0.914	0.917	0.921	0.916	0.918	0.917	0.919
	Macro-F1	0.706	0.709	0.721	0.708	0.712	0.707	0.707
	AUC	0.851	0.860	0.867	0.860	0.858	0.858	0.844
Bitcoin-OTC	Micro-F1	0.897	0.897	0.901	0.897	0.895	0.899	0.892
	Macro-F1	0.767	0.767	0.773	0.764	0.762	0.769	0.751
	AUC	0.884	0.883	0.886	0.880	0.880	0.880	0.877
Slashdot	Micro-F1	0.888	0.891	0.887	0.885	0.890	0.887	0.880
	Macro-F1	0.757	0.765	0.759	0.758	0.757	0.755	0.728
	AUC	0.906	0.907	0.900	0.899	0.903	0.902	0.881
Epinions	Micro-F1	0.920	0.919	0.918	0.917	0.915	0.914	0.901
	Macro-F1	0.902	0.901	0.900	0.898	0.896	0.895	0.880
	AUC	0.966	0.965	0.964	0.964	0.964	0.963	0.951

TABLE IX
THE EFFECT OF β ON SIGN PREDICTION ACCURACIES OF TRUSTSGCN WHEN WE SET x TO 80

Datasets	Metrics	$\beta=0.2$	$\beta=0.4$	$\beta=0.6$	$\beta=0.8$	$\beta=0.9$	$\beta=0.95$	$\beta=0.96$	$\beta=0.97$	$\beta=0.98$	$\beta=0.99$	$\beta=1$
Bitcoin-Alpha	Micro-F1	0.913	0.917	0.914	0.921	0.919	0.917	0.917	0.917	0.913	0.914	0.919
	Macro-F1	0.689	0.698	0.695	0.721	0.712	0.704	0.717	0.711	0.689	0.710	0.705
	AUC	0.853	0.852	0.854	0.867	0.866	0.860	0.858	0.859	0.860	0.859	0.861
Bitcoin-OTC	Micro-F1	0.890	0.892	0.891	0.894	0.895	0.901	0.893	0.891	0.892	0.899	0.897
	Macro-F1	0.745	0.748	0.751	0.751	0.758	0.773	0.751	0.747	0.748	0.768	0.756
	AUC	0.875	0.876	0.872	0.873	0.874	0.886	0.883	0.884	0.884	0.881	0.883
Slashdot	Micro-F1	0.877	0.876	0.880	0.869	0.868	0.875	0.870	0.884	0.886	0.881	0.891
	Macro-F1	0.721	0.713	0.719	0.689	0.683	0.700	0.682	0.734	0.736	0.727	0.765
	AUC	0.888	0.885	0.885	0.887	0.889	0.887	0.889	0.901	0.904	0.900	0.907
Epinions	Micro-F1	0.911	0.914	0.915	0.911	0.914	0.906	0.911	0.913	0.915	0.914	0.920
	Macro-F1	0.891	0.894	0.896	0.891	0.894	0.882	0.891	0.893	0.896	0.895	0.902
	AUC	0.960	0.962	0.962	0.961	0.961	0.960	0.961	0.962	0.963	0.962	0.966

formed by the combination of four possible sign pairs and four possible direction pairs that the two edges can have.

APPENDIX B FURTHER RESULTS

Further Results for EQ1-2. In (M3) of TrustSGCN, we employ a sampling strategy to improve both training efficiency and accuracy. In addition to Figure 5, Table VIII shows the accuracy changes according to the number of randomly sampled nodes (*i.e.*, γ). We can see that using this sampling strategy is more effective than not using the strategy at all.

Further Results for EQ4. In (M2) of TrustSGCN, we verify whether $Trust(\hat{s}_{ij})$ exceeds the predefined threshold β , *i.e.*, the second condition for determining the trustworthiness of edge signs. In addition to the AUC results (*i.e.*, Figure 6), we also provide the results for other metrics in Table IX. Similar to Figure 6, we can see that TrustSGCN is more accurate when the value of β is relatively large.